Received: 30 January 2017 | Accepted: 25 February 2017

DOI: 10.1111/gcb.13771

PRIMARY RESEARCH ARTICLE

WILEY Global Change Biology

# A common thermal niche among geographically diverse populations of the widely distributed tree species *Eucalyptus tereticornis*: No evidence for adaptation to climate-of-origin

John E. Drake[1] | Angelica Vårhammar[1] | Dushan Kumarathunge[1] | Belinda E. Medlyn[1] | Sebastian Pfautsch[1] | Peter B. Reich[1,2] | David T. Tissue[1] | Oula Ghannoum[1] | Mark G. Tjoelker[1]

[1]Hawkesbury Institute for the Environment, Western Sydney University, Penrith, NSW, Australia

[2]Department of Forest Resources, University of Minnesota, St. Paul, MN, USA

**Correspondence**
John E. Drake, Hawkesbury Institute for the Environment, Western Sydney University, Penrith, NSW, Australia.
Email: je.drake@westernsydney.edu.au

**Funding information**
Australian Research Council, Grant/Award Number: DP140103415

## Abstract

Impacts of climate warming depend on the degree to which plants are constrained by adaptation to their climate-of-origin or exhibit broad climatic suitability. We grew cool-origin, central and warm-origin provenances of *Eucalyptus tereticornis* in an array of common temperature environments from 18 to 35.5°C to determine if this widely distributed tree species consists of geographically contrasting provenances with differentiated and narrow thermal niches, or if provenances share a common thermal niche. The temperature responses of photosynthesis, respiration, and growth were equivalent across the three provenances, reflecting a common thermal niche despite a 2,200 km geographic distance and 13°C difference in mean annual temperature at seed origin. The temperature dependence of growth was primarily mediated by changes in leaf area per unit plant mass, photosynthesis, and whole-plant respiration. Thermal acclimation of leaf, stem, and root respiration moderated the increase in respiration with temperature, but acclimation was constrained at high temperatures. We conclude that this species consists of provenances that are not differentiated in their thermal responses, thus rejecting our hypothesis of adaptation to climate-of-origin and suggesting a shared thermal niche. In addition, growth declines with warming above the temperature optima were driven by reductions in whole-plant leaf area and increased respiratory carbon losses. The impacts of climate warming will nonetheless vary across the geographic range of this and other such species, depending primarily on each provenance's climate position on the temperature response curves for photosynthesis, respiration, and growth.

**KEYWORDS**
acclimation, autotrophic respiration, climate change, *Eucalyptus tereticornis*, forest red gum, local adaptation, photosynthesis, temperature

## 1 | INTRODUCTION

Climate warming has the potential to create a mismatch between forest trees and their "home" environments to which they have adapted for centuries or millennia (Davis & Shaw, 2001; Doak & Morris, 2010; Jump & Penuelas, 2005). Under the current trajectory, further greenhouse warming of 2.6 to 4.8°C is projected by 2100, exceeding both the magnitude and rate of climatic change throughout the last 1,400 years (RCP 8.5, Collins et al., 2013). Given that trees cannot migrate fast enough to escape increased temperatures,

  

a growing mismatch is expected between trees, their climatic optima and tolerance limits as climate warming drives shifts in suitable geographic ranges (González-Orozco et al., 2016; Loarie et al., 2009; Parmesan, 2006; Woodward, 1987).

Widespread tree species exhibit substantial biogeographic variation, reflecting a mix of local adaptation and phenotypic plasticity across a range of climatic conditions (e.g., Rehfeldt, Wykoff, & Ying, 2001; Rehfeldt, Ying, Spittlehouse, & Hamilton, 1999; Rehfeldt et al., 2002; Valladares et al., 2014). Local adaptation of tree species to climate is not only restricted to species with narrow native geographic distributions, but also occurs in widely distributed species (Davis & Shaw, 2001). In forest trees, geographic provenances (i.e., seed sources) within widely distributed species have long been recognized as an important source of structured genetic variation along climate gradients (Langlet, 1936; Rehfeldt et al., 2002; Reich & Oleksyn, 2008). Evidence for this generalization largely arises from observations of temperate and boreal taxa, particularly conifers of the Northern Hemisphere (Alberto et al., 2013). Common garden trials reveal biogeographic patterns in plant traits among provenances that are frequently arrayed along latitudinal and elevational clines, and interpreted as climate-related genetic variation (Alberto et al., 2013; Rehfeldt et al., 1999, 2001, 2002; Reich & Oleksyn, 2008). However, the generality of these patterns among other taxa, particularly those of the low-latitudes and tropics, remains an open question. Likewise, the role of trait plasticity and adaptive fitness among populations within species is less well understood (Valladares et al., 2014).

Eucalypts are largely outcrossing species with limited dispersal ability and comparatively high levels of genetic variation within as well as among populations (Dillon et al., 2014; Moran, 1992; Potts & Wiltshire, 1993). Geographic patterns of quantitative genetic variation in eucalypts are often complex, arising through effects of migration, selection and genetic drift that may vary in time and space. Genetic variation in traits among provenances has been observed in widely distributed eucalypts along rainfall (McLean et al., 2014) and altitudinal clines (Gauli, Vaillancourt, Bailey, Steane, & Potts, 2015; Slatyer & Ferrar, 1977) and noted in forestry provenance trials worldwide (Booth et al., 2015), suggesting that widely distributed eucalypts may exhibit structured intraspecific geographic variation in functional traits in relation to climate-of-origin.

*Eucalyptus tereticornis* is a common and widely distributed tree species along the eastern coast of Australia, with a native range spanning ~2,500 km and ~13°C in mean annual temperature (MAT) from temperate climates in the south to tropical climates in the north (MAT from 13 to 26°C; bio1 data from bioclim; Busby, 1991). We previously found that 12 diverse seed sources of this species differed in response to experimental warming of 3.5°C relative to their home climate-of-origin in a manner that depended on their geographic origin. Warming increased photosynthetic capacity, leaf area and growth in cool-origin provenances, whereas an opposite effect was observed in warm-origin provenances, which exhibited reduced photosynthetic capacity, leaf area, and growth (Drake et al., 2015).

While this climate shift experiment revealed responses of functional traits to directional warming along an array of home temperatures spanning the native range of the species, it is not clear whether this was the result of underlying genetic differences in provenances arrayed along this climate gradient. One possibility is that functional traits of provenances responded to warming in a manner that reflect differentiated or narrowed thermal niches relative to the climate envelope of the species (Figure 1a). This scenario would reflect genetic differentiation among provenances (i.e., local adaptation) that restricted trait plasticity across wide-ranging thermal environments. This hypothesis was deemed most likely, given that local adaptation within tree species is commonly reported in the literature (Alberto et al., 2013; Rehfeldt et al., 1999, 2001, 2002; Reich & Oleksyn, 2008). Alternatively, provenances might exhibit trait responses to warming that reflect a shared, broad fundamental thermal niche that effectively spans the entire native geographic range of the species (Figure 1b). This scenario would reflect little underlying genetic differentiation and broad physiological and morphological plasticity, with positive trait responses to warming at temperatures below the optima and negative responses at temperatures above the optima. These scenarios have different consequences for predicting responses to climate warming in a widely distributed species (Davis & Shaw, 2001; Valladares et al., 2014). Local adaptation could lead to reduced capacity to respond to climate warming among provenances throughout the climatic range of the species, whereas broad phenotypic plasticity in functional traits would act as a buffer against directional climatic selection.

These alternative scenarios (i.e., differentiated narrow vs. undifferentiated broad thermal niches) for functional traits of provenances of contrasting geographic origins (i.e., cool-origin, central and warm-origin) can be resolved experimentally by growing each provenance in an array of common temperature environments that span the thermal range of the species. We designed such an experiment with *E. tereticornis* to test the following alternative hypotheses: (i) if limitations to long-distance gene flow combined with directional selection across large geographic space allowed for genetic adaptation to

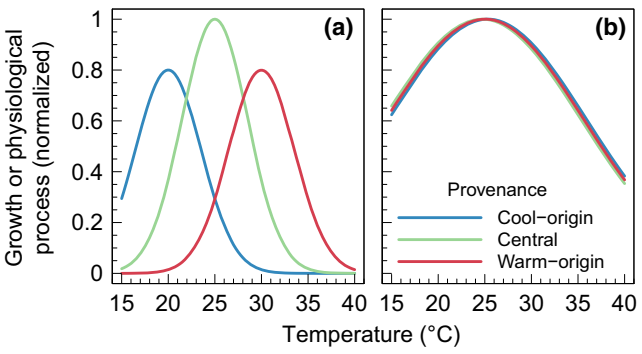


**FIGURE 1** Conceptual depiction of three provenances of a widely distributed species with (a) strong local adaptation and divergence in thermal physiology, or (b) limited local adaptation with a broad and common fundamental thermal niche. These are contrasting examples- many other possibilities exist

local climate conditions, then we will observe divergent responses of photosynthesis, respiration and growth to temperature across provenances of this species (different curves, Figure 1a); (ii) alternatively, if gene flow among provenances of this widely distributed species was maintained or climatic selection was relatively weak in comparison to extant local genetic variation, then we will observe equivalent responses of photosynthesis, respiration and growth across provenances (common curves, Figure 1b). We also quantified key traits underpinning plant growth and function, using classical growth analysis techniques to provide a framework for integration of physiological and morphological traits in a whole-plant context (Poorter, Remkes, & Lambers, 1990). We define the physiological thermal niche in terms of growth-temperature response functions of $CO_2$ exchange rates, growth rate, and underlying traits.

## 2 | MATERIALS AND METHODS

### 2.1 | Experimental design

Three provenances of the widely distributed Forest Red Gum (*E. tereticornis* sp. *tereticornis*) were selected to represent cool-origin, central, and warm-origin locations within the species' distribution (Figure 2). Seeds from each provenance were obtained from the Australian Tree Seed Centre (CSIRO Canberra, Australia; seedlot numbers 17770, 20352, and 18589). The cool-origin provenance originated from southern New South Wales, Australia, near Bateman's Bay (35°23′60″S, 150°4′12″E), where the mean annual temperature (MAT) is ~13°C. The central provenance originated in southern Queensland, near Brisbane (26°34′12″S, 152°0′36″E) where MAT is ~22°C, ~1,000 km north of the cool-origin provenance. The warm-origin provenance originated in northern Queensland, near Port Douglas (15°30′0″S, 145°8′24″E), where MAT is ~26°C, ~1,400 km north-northwest of the central provenance and ~2,200 km north of the cool-origin provenance. These are a subset of the 12 provenances studied by Drake et al. (2015; Figure 2).

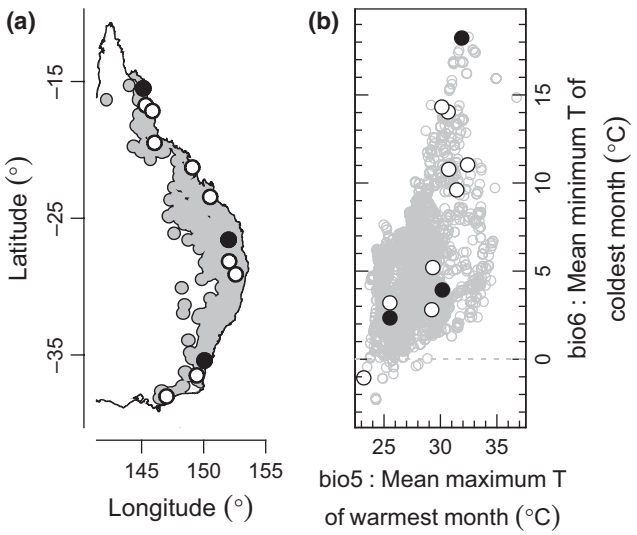


**FIGURE 2** The distribution of *Eucalyptus tereticornis* in geographic (a) and climate space (b). Grey symbols reflects the species' native range as measured by occurrence records in the Atlas of Living Australia (a) and associated worldclim climate data (b). White and black circles together denote provenances studied by Drake et al. (2015). Three of those provenances were selected and studied here; these are denoted by black circles

We implemented six temperature treatments in six adjacent rooms (8 m long × 3 m wide × 5 m tall) in a naturally lit, controlled environment glasshouse (Plexiglas Alltop SDP 16; Evonik Performance Materials, Darmstadt, Germany) at Western Sydney University (Richmond, NSW, Australia). The temperature treatments were designed to span the entire range of average summer temperatures experienced by *E. tereticornis* in its native range, plus two additional high-temperature treatments that reflect temperatures outside its native range. The mean daily temperatures for the six treatments were set to 18, 21.5, 25, 28.5, 32, and 35.5°C; these temperatures were achieved across the experiment (Fig. S1). The average summer temperatures at seed-origin (i.e., "home") were approximated by the 18°C treatment for the cold-origin provenance (room 1), the 21.5°C treatment for the central provenance (room 2), and the 28.5°C treatment for the warm-origin provenance (room 4; Drake et al., 2015). A typical diurnal range of ~9°C was maintained in all treatments via ten temperature set points throughout the day-night cycle (Automated Logic WebCTRL Building Management System; Braemar Th320 Natural gas heater; Dunnair PHS25 Air Conditioner, using Vaisala HMP110 Humidity/Temperature probes and HMT130 Transmitters). Relative humidity was kept above 50% (Carel Humidisk 65 humidifier), but vapor pressure deficit (VPD) increased with growth temperature, as expected (Fig. S1). Thus, we recognize that VPD may have contributed, in part, to several of the temperature dependencies discussed in this work. The photosynthetic photon flux density (PPFD) at canopy height (Apogee quantum sensor, USA) varied with prevailing weather conditions but was equivalent across rooms (ANOVA; $p = .98$; Fig. S1d). Daytime maximum PPFD was often ~1,500 μmol $m^{-2}$ $s^{-1}$ (Fig. S1d).

Seeds were germinated in a shadehouse over a period of 8 weeks (Greening Australia, Richmond, Australia) after which seedlings (~13 cm in height) were transplanted individually into 7 L pots. A sandy clay loam was sourced from the same local quarry as used previously (Drake et al., 2015; Menangle, NSW, Australia). The soil was a moderately fertile sandy loam: pH = 4.3 (0.01 M CaCl), organic carbon content = 1.2%, total Kjeldahl $N$ = 520 mg $kg^{-1}$, total P = 230 mg $kg^{-1}$, Ca = 17 mg $kg^{-1}$, Mg = 13 mg $kg^{-1}$, Na = 30 mg $kg^{-1}$, K = 30 mg $kg^{-1}$ (ALS Laboratory Group, Smithfield, NSW, Australia). All seedlings were measured for basal diameter and height, and 15 seedlings of each provenance were assigned to each of the six temperature treatments in a stratified random design. Potted trees were moved into their temperature treatments during the Austral summer on 8 Jan 2016; we define this as day zero.

All trees were kept well-watered with an automated irrigation system and were fertilized fortnightly with a liquid fertilizer (250 mL Aquasol, at 1.6 g $L^{-1}$; 23% N, 4% P, 18% K, 0.05% Zn, 0.06% Cu,

0.0013% Mo, 0.15% Mn, 0.06% Fe, 0.011% B, Yates Australia, Padstow, NSW, Australia). Soil volumetric water content (VWC) was measured hourly for four trees in each room using time-domain reflectometers installed vertically into each pot (CS650; Campbell Scientific, Logan, UT, USA). The field capacity of this soil was approximately 0.25 $m^3\ m^{-3}$ and the permanent wilting point was approximately 0.05 $m^3\ m^{-3}$ (established with unwatered plant-free pots), while VWC was maintained at approximately 0.15 $m^3\ m^{-3}$ throughout the experiment. During the growth interval (*see below*), VWC was an average of 0.19 $m^3\ m^{-3}$ and did not vary across temperature treatments. Pre-dawn leaf water potential ($\Psi_{pd}$) was measured for five trees in each room on 24 Feb 2016 with a using a Scholander-type pressure chamber (1505D-EXP; PMS Instrument Company, OR, USA); mean $\Psi_{pd}$ ranged from −0.2 to −0.6 MPa. These VWC and $\Psi_{pd}$ results indicate that the trees were not stressed by low water availability in any of the temperature treatments. To minimize the effects of any potential unmeasured environmental heterogeneity within the glasshouse, the treatments were randomly allocated to the six rooms and reallocated a second time after 10 days. The seedlings were also randomly rotated within rooms throughout the experiment.

## 2.2 | Leaf-scale physiology

A fully developed leaf that had formed during the temperature treatment was selected and marked on eight seedlings per provenance and treatment combination; these leaves were used for measurements of light-saturated photosynthesis at in-situ growth temperatures ($A_{sat}$), the short-term temperature dependence of light saturated photosynthesis ($A_{sat}$−T), and the short-term temperature dependence of leaf dark respiration ($R_{dark}$−T). $A_{sat}$ is a measure of performance of the three provenances across all six growth environments, while $A_{sat}$−T and $R_{dark}$−T focus on contrasting the three provenances grown in a single growth environment (i.e., a common garden), such that any provenance differences in short-term temperature responses could be attributable to underlying genetic differences.

We measured $A_{sat}$ at the in-situ growth temperature over 2 days (days 26 and 27) during the 11-day growth interval (*see below*) using six cross-calibrated portable open flow photosynthesis systems equipped with LED light sources and the standard 2 × 3 cm chambers (Li-6400-XT and Li-6400-02B LED, Licor Biosciences, Lincoln, NE, USA). These measurements were performed on all eight seedlings per provenance and treatment combination (8 seedlings × 3 provenances × 6 growth environments = 144 measurements). Measurements were completed using a flow rate of 500 μmol $s^{-1}$ and a relative humidity between 65 and 80%. The photosynthetic photon flux density (PPFD) was set to 1500 μmol $m^{-2}s^{-1}$ and the $CO_2$ concentration in the sample cell was adjusted to 400 ± 5 ppm by manipulating the $CO_2$ concentration of the reference cell. Temperature targets were set relative to the mid-morning temperature in each treatment (i.e., 20, 24, 28, 32, 36, and 40°C). Leaf temperatures were controlled to be within ±1.5°C of the target temperature by manually adjusting the temperature of the chamber block. We measured $A_{sat}$ at 1500 μmol $m^{-2}s^{-1}$ PPFD, given that rates of $A_{net}$ were saturated at this PPFD (JE Drake, personal observation of >100 light response curves) and the rarity of PPFD conditions above 1500 μmol $m^{-2}\ s^{-1}$ (Fig. S1d).

We also measured the direct short-term temperature response of $A_{sat}$ ($A_{sat}$−T) on day 29 using seedlings from a single growth temperature treatment only (21.5°C; 8 seedlings × 3 provenances × 6 measurement temperatures = 144 measurements). For this subset, the seedlings were moved among treatment rooms and measured at all six temperatures. A minimum wait period of 20 min allowed the seedlings to adjust to the new temperature before measurement. As this day was cloudy with low incident PPFD, plants were light-acclimated at a PPFD of ~1000 μmol $m^{-2}\ s^{-1}$ using growth lamps (Lumigrow Pro 650, Lumigrow Inc., Emeryville, CA, USA) for a minimum of 20 min prior to measurement.

We measured the short-term temperature dependence of leaf dark respiration ($R_{dark}$−T) between 22:00 and 02:00 h on the night between days 35 and 36. $R_{dark}$ was measured at five night-time temperature targets (14, 18, 22, 26, and 30°C) using five Li-6400-XT equipped with conifer chambers (Li-6400-22; Licor). Measurements were completed using a flow rate of 300 μmol $s^{-1}$, relative humidity between 65 and 80%, and a reference $CO_2$ concentration of 400 ppm. Leaf temperature was controlled to within ±1°C of the target temperature by adjusting the block temperature. The cuvette was covered by a cloth to ensure dark conditions during measurements. Leaves were removed, scanned for leaf area using a leaf area meter (Li-3100C, Licor), placed in moist zip-locked bags, and moved among treatment rooms for measurement. Each leaf was allowed to adjust to each treatment temperature for at least 20 min in a darkened box before measurements commenced. Leaves were subsequently dried and weighed, facilitating the expression of $R_{dark}$ on an area- or mass-basis ($R_{area}$ and $R_{mass}$). Measuring $R_{dark}$ on detached leaves is common (e.g., Atkin et al., 2015; Bolstad, Reich, & Lee, 2003; Davey et al., 2004; Reich et al., 2016) and well supported by studies that measured $R_{dark}$ on attached and detached leaves and found equivalent and stable rates for at least several hours (Mitchell, Bolstad, & Vose, 1999; O'Sullivan et al., 2013; Reich et al., 1998). Furthermore, we expect any effect of leaf removal to be systematic and not affect our ability to resolve differences among the provenances.

## 2.3 | Whole-plant respiration

We measured the tissue-specific rates of leaf, stem (including branch), and root respiration at a common temperature of 25°C for five harvested plants per provenance per growth temperature between days 41 and 48 (3 provenances × 6 temperatures × 5 replicate seedlings × 3 organs = 270 measurements; Li-6400-XT with Li-6400-22 conifer chambers; Licor). These measurements enabled investigation of acclimation of respiration via the set temperature method (Atkin, Bruhn, & Tjoelker, 2005). We removed all of the leaves of each tree and measured total leaf area (Li-3100C,

Licor). We compiled the stem and branches into a composite sample for each tree. We isolated the root system of every plant using a washing station and sieves (2 mm). We randomly selected three leaves and pooled them together for an aggregate measure of respiration ($R_{leaf}$). We cut the stem and branches into ~5 cm segments and measured the entire aggregate sample ($R_{stem}$). We isolated the roots from soil using the washing station, removed excess moisture by blotting with paper towel, and measured either the entire, intact root system or a subsample of ca. half the root system ($R_{root}$). The block temperature was controlled such that the tissue temperature was 25 ± 1.5°C. The $CO_2$ concentration of the reference cell was 400 ppm. Typically, a flow rate of 400 μmol $s^{-1}$ was used; this flow rate was increased to 600 or 700 μmol $s^{-1}$ for root systems that were releasing a large amount of water vapor. All samples were oven dried and weighed. We recognize that $CO_2$ dissolved in the xylem stream could have been released during the stem measurements and that sampling may have affected respiratory rates. However, measuring respiratory components of detached plant organs is a standard approach (e.g., Poorter et al., 1990; Tjoelker, Oleksyn, & Reich, 1999; Tjoelker, Craine, Wedin, Reich, & Tilman, 2005; Comas & Eissenstat, 2004), and we expect any associated effects to be systematic across provenances and not affect our ability to detect provenance differences. Total plant respiration in each temperature treatment was estimated from the $R_{leaf}$, $R_{stem}$, and $R_{root}$ measurements, assuming all organs shared a common short-term temperature response as measured for leaves (Equation [3], *see below*).

## 2.4 | Growth analysis

We tracked growth via measurement of basal diameter (d; mean of two perpendicular measures) and height of the main stem (h). We harvested trees periodically throughout the study to develop an allometric relationship between tree size (diameter$^2$ × height; $d^2$ h) and total mass (Fig. S2). This included 10 seedlings per provenance at the start of the experiment and 12 trees per provenance in each treatment throughout the study, including those harvested for respiration measurements. We removed all the leaves for a bulk measurement of total leaf area (Li-3100C, Licor) and dry mass, and compiled the stem and branches for a measurement of aboveground woody mass. We isolated the root system of every plant using a washing station and sieves (2 mm); these roots were oven-dried and weighed. In total, we harvested 156 plants to develop the relationship between size ($d^2$ h) and total mass (sum of leaf, stem and branches, and root mass; Fig. S2; $\log_{10}(\text{total mass}) = -0.018 + 0.85(\log_{10}(d^2\ h)) - 0.064(\log_{10}(d^2\ h))^2$; $r^2 = .98$).

The height and diameter measurements allowed calculation of total mass and growth rates of individual plants. To investigate the drivers of growth in a relative growth rate context (Poorter et al., 1990; Shipley, 2006), we focused on an 11-day growth interval between days 21 and 32 in which we tracked the growth of 15 seedlings per provenance and treatment. We identified this growth interval a priori, given the importance of early growth responses for experiments with seedlings (e.g., Kirschbaum, 2011). Mean relative growth rate (RGR; g $g^{-1}$ $d^{-1}$) over the 11-day interval is related to leaf area ratio (LAR; ratio of leaf area to total plant mass) and net assimilation rate (NAR; g $m^{-2}$ $g^{-1}$; Shipley, 2006; Equation [1]).

$$RGR = LAR \times NAR \quad (1)$$

LAR can be further subdivided into the product of leaf mass fraction (LMF; ratio of leaf mass to total plant mass) and specific leaf area (SLA; $m^2$ $g^{-1}$). We measured SLA by collecting three or four leaf punches (0.69 $cm^2$; avoiding the midvein) from each seedling at the start and the end of the interval, which we then dried at 70°C and weighed. We determined the total leaf area for each seedling at the beginning and end of the growth interval by counting the leaves, divided into two size categories (small, from 3 to 5 cm in length, and large, >5 cm in length). We measured the size ($cm^2$) of one leaf of each category on each seedling using a hand-held leaf area meter (Li-3000, Licor). We calculated the total leaf area of each tree as the product of leaf number and leaf size, summed for the two leaf categories. We evaluated this method with 48 plants that were harvested on the following day, revealing a strong relationship between the directly measured and estimated total crown leaf area ($y = 51.8 + 0.64x$, $r^2 = .94$, $p < .001$).

## 2.5 | Fitting temperature response curves

We fit mathematical models to derive parameter estimates describing the temperature responses of measured variables. We used the equation of June, Evans, and Farquhar (2004) for many measurements, as this simple equation with only three parameters explained the data well. This equation is:

$$P(T_i) = P(T_o)e^{-\left(\frac{T_i - T_o}{\Omega}\right)^2} \quad (2)$$

where $P(T_i)$ is the process rate at the in-situ temperature $T_i$, $P(T_o)$ is the process rate at the optimum temperature $T_o$, and Ω is the difference in temperature from $T_o$ where the process rate falls to $e^{-1}$ of its value at $T_o$ (i.e., the temperature difference from $T_o$ where the rate falls to 37% of its rate at $T_o$). Large values of Ω reflect broad temperature-response curves, while small values of Ω reflect narrow curves. This equation assumes that the process rate is symmetric around $T_o$, which appears to be appropriate for the data presented here.

The $R_{dark}$ data were exponential and did not show a distinct peak, so we fit these data with a $Q_{10}$ function:

$$R(T) = R(T_{ref})Q_{10}^{\frac{T - T_{ref}}{10}} \quad (3)$$

where $R(T)$ is the rate of $R_{dark}$ at temperature $T$, $R(T_{ref})$ is the rate of $R_{dark}$ at a reference temperature $T_{ref}$, and $Q_{10}$ is the multiplicative rate of increase in $R_{dark}$ for every 10°C change in temperature. We adopted a $T_{ref}$ value of 22°C to fit the $R_{dark}$ data, as this was the intermediate measurement temperature. Recent work has challenged the use of such "constant $Q_{10}$" models, particularly for describing high-resolution $R_{dark}$-T measurements (Heskel et al., 2016), as the

$Q_{10}$ often declines with temperature (Tjoelker, Oleksyn, & Reich, 2001). We follow Reich et al. (2016) and use Equation (3) to fit our relatively coarse $R_{dark}$–T relationships, as this simple function with only two parameters described the data well. Simple linear models were used instead of Equations (2) and (3) for the temperature dependence of net assimilation rate and leaf mass fraction, as Equations (2) and (3) were not appropriate to describe these data.

### 2.6 | Data analysis

We considered the unit of replication to be the tree ($n$ = 5 to 15 trees per provenance per growth environment, depending on the response variable). All data were analyzed in *R* version 3.3.2 (R Development Core Team, 2012). Temperature response curves (Equations [2] and [3]) were fit to the data for each provenance within each growth environment using the "nls" function within the "stats" package, and 95% confidence intervals for each parameter were calculated with the "confint2" function within the "nlstools" package (Baty et al., 2015). These 95% confidence intervals were used to make inferences regarding differences in the temperature responses across provenances.

The inferences based on confidence intervals were supplemented with traditional inferential statistics based on non-linear mixed-effects models (NLMMs, hereafter) utilizing the "nlme" *R* package. Specifically, we tested whether temperature-response parameters (Tables 1 and 2) varied significantly across the three provenances. We fit mixed-effects models that did and did not contain a fixed provenance effect for the parameter of interest (e.g., $T_{opt}$ of AGR); these models were then compared by likelihood ratio tests to determine the probability that provenance values significantly differed from each other. Thus, the null model contained no fixed effects, while the alternate model contained a single fixed effect of provenance with three levels for the response variable of interest. A random provenance effect was included for the process rate at the optimal or reference temperature, except when this process rate was the variable of interest; in these cases, a random provenance effect on $T_{opt}$ or $Q_{10}$ was included. When this test indicated that the model including a fixed provenance effect was a significant improvement over the null model, we tested provenance pairwise comparisons using post-hoc tests as implemented in the "multicomp" *R* package.

The entire analysis presented here is reproducible; all of the raw data are available as a published data product (Drake, Vårhammar, et al., 2016) and code to reproduce all of the analysis, figures, and tables are available as a *git* repository (https://github.com/jedrake/GREAT).

## 3 | RESULTS

### 3.1 | Photosynthesis

Rates of leaf-level photosynthesis at saturating light and the in-situ growth temperature ($A_{sat}$) showed a peaked relationship with leaf temperature that was equivalent across all three provenances (Figure 3). The $T_{opt}$ of $A_{sat}$ was 28.8°C and did not differ between provenances (Figure 3, Table 1). Notably, the 95% confidence intervals of all parameters overlapped for all three provenances (Table 1). NLMMs indicated that the central provenance had a higher rate of $A_{sat}$ at $T_{opt}$ and a larger Ω than the cool- or warm-origin provenances (Table 1; $A_{sat}$ in situ), although these differences were small (Figure 3). The lack of strong provenance differences in the temperature dependence of $A_{sat}$ is consistent with the second hypothesis of limited differentiation in thermal physiological traits.

We also measured the short-term temperature dependence of $A_{sat}$ for plants grown in the 21.5°C environment to determine whether provenances also shared a common short-term temperature response of $A_{sat}$. Indeed, provenances had similar short-term $A_{sat}$–T dependences with a common $T_{opt}$ of ~29°C, in agreement with the in-situ $T_{opt}$ measurements (Fig. S3; Table 1). Although the cool-origin provenance had a lower rate of $A_{sat}$ relative to the other provenances in this measured subset of plants (Table 1), all three provenances displayed equivalent temperature dependencies of in-situ $A_{sat}$ and did not differ in $T_{opt}$ or Ω for short-term measurements $A_{sat}$. We conclude that there is little evidence of provenance differences in $A_{sat}$ and its temperature dependence, consistent with the hypothesis 2.

### 3.2 | Respiration

All provenances exhibited equivalent short-term temperature-responses of leaf $R_{dark}$ (Fig. S4, Table 2). For both mass- and area-based $R_{dark}$, provenances had overlapping 95% CIs for both the basal rates of $R_{dark}$ at a reference temperature of 22°C and the $Q_{10}$ values (Table 2). Furthermore, NLMMs indicated no significant difference in any parameter value regarding the temperature dependence of mass- or area-based $R_{dark}$ (Table 2).

Tissue specific rates of leaf, stem, and root respiration measured at a common temperature of 25°C declined in an asymptotic manner with increasing growth temperature (Figure 4a–c). Specific respiration rates were remarkably similar across organs; $R_{leaf}$, $R_{stem}$, and $R_{root}$ measured at 25°C declined from ~25 nmol $g^{-1}$ $s^{-1}$ in the coldest growth temperature to ~15 nmol $g^{-1}$ $s^{-1}$ at any growth temperature exceeding 25°C (Figure 4a–c). This decline in $R_{dark}$ at a common measurement temperature reflects respiratory acclimation to growth temperature (Atkin et al., 2005). The lack of change in $R_{leaf}$, $R_{stem}$, and $R_{root}$ (measured at 25°C) for plants at growth temperatures exceeding 25°C may reflect a constraint on respiratory acclimation at high temperature.

We estimate the tissue-specific rates of leaf, stem, and root respiration at the in-situ growth temperatures (Figure 4d–f) given the measured rates at 25°C and the short-term temperature dependence of leaf respiration (Fig. S4). Leaf, stem, and root respiration at in-situ growth temperatures did not vary appreciably between 18 and 25°C (Figure 4d–f). That is, respiratory acclimation was approximately homeostatic across this temperature range. However at growth temperatures exceeding 25°C, the lack of acclimation (Figure 4a–c) led to an increase in the tissue-specific rate of in-situ

**TABLE 1** Temperature-response parameter estimates and 95% confidence intervals for measures of growth and photosynthesis for three provenances of *E. tereticornis* based on Equation (2). Statistically significant differences in parameters across provenances are indicated by different capital letters

| Variable | Location[a] | $T_o$ (°C)[b] | $P(T_o)$[c] | Ω (°C)[d] |
|---|---|---|---|---|
| $A_{sat}$ (in situ)[j] | Cool-origin | 28.5 (26.6–29.8)$^A$ | 23.6 (21.9–25.4)$^A$ | 16.8 (13.9–22.3)$^A$ |
| $A_{sat}$ (in situ) | Central | 28.8 (27.6–29.8)$^A$ | 26.1 (24.7–27.5)$^B$ | 17.6 (15.2–21.5)$^B$ |
| $A_{sat}$ (in situ) | Warm-origin | 29.1 (28.3–29.9)$^A$ | 25.5 (24.3–26.8)$^A$ | 15.3 (13.7–17.6)$^A$ |
| $A_{sat}$ (A-T)[k] | Cool-origin | 29.0 (28.0–29.8)$^A$ | 25.0 (24.1–26.0)$^A$ | 21.1 (18.7–24.6)$^A$ |
| $A_{sat}$ (A-T) | Central | 29.2 (28.7–29.7)$^A$ | 28.4 (27.7–29.0)$^B$ | 21.0 (19.5–22.9)$^A$ |
| $A_{sat}$ (A-T) | Warm-origin | 28.3 (27.5–29.1)$^A$ | 29.3 (28.6–30.0)$^B$ | 20.8 (19.0–23.3)$^A$ |
| Final mass[e] | Cool-origin | 28.9 (27.3–31.4)$^A$ | 9.6 (7.8–11.5)$^A$ | 9.8 (7.4–15.3)$^A$ |
| Final mass | Central | 28.3 (26.7–30.5)$^A$ | 8.1 (6.5–9.9)$^A$ | 9.4 (7.2–14.4)$^A$ |
| Final mass | Warm-origin | 28.3 (26.8–30.1)$^A$ | 9.2 (7.3–11.1)$^A$ | 8.6 (6.6–12.2)$^A$ |
| AGR[f] | Cool-origin | 28.3 (27.8–28.8)$^A$ | 0.38 (0.36–0.41)$^A$ | 8.3 (7.8–9.1)$^A$ |
| AGR | Central | 28.0 (27.5–28.5)$^A$ | 0.36 (0.33–0.38)$^A$ | 8.1 (7.4–9.0)$^A$ |
| AGR | Warm-origin | 27.7 (27.1–28.2)$^A$ | 0.35 (0.32–0.37)$^A$ | 8.5 (7.7–9.5)$^A$ |
| RGR[g] | Cool-origin | 24.3 (23.5–24.9)$^A$ | 0.12 (0.12–0.13)$^A$ | 12.0 (10.8–13.6)$^A$ |
| RGR | Central | 24.4 (23.5–25.2)$^A$ | 0.12 (0.12–0.13)$^A$ | 13.0 (11.6–15.1)$^A$ |
| RGR | Warm-origin | 24.8 (24.0–25.5)$^A$ | 0.12 (0.12–0.13)$^A$ | 13.1 (11.7–15.0)$^A$ |
| LAR[h] | Cool-origin | 27.5 (26.6–28.4)$^A$ | 14.2 (13.0–15.4)$^A$ | 12.0 (9.9–14.0)$^A$ |
| LAR | Central | 26.7 (25.2–28.3)$^A$ | 11.7 (10.8–12.6)$^B$ | 18.0 (12.9–23.2)$^A$ |
| LAR | Warm-origin | 29.0 (27.8–30.2)$^A$ | 14.9 (13.6–16.2)$^A$ | 12.8 (10.3–15.4)$^A$ |
| SLA[i] | Cool-origin | 29.8 (28.8–30.9)$^A$ | 481 (464–498)$^A$ | 17.1 (14.7–19.5)$^A$ |
| SLA | Central | 28.5 (27.8–29.2)$^B$ | 432 (418–446)$^B$ | 16.8 (14.9–18.7)$^A$ |
| SLA | Warm-origin | 28.9 (28.0–29.7)$^A$ | 480 (464–495)$^A$ | 18.1 (15.8–20.5)$^A$ |

[a]Provenances were from the cool-origin, central, or warm-origin regions of the species' distribution.
[b]The temperature optimum of a process (°C).
[c]Process rate at the optimal temperature. Units varied across response variables.
[d]The breadth of the temperature-response; the difference in temperature from $T_o$ at which the process rate falls to $e^{-1}$ of its value at $T_o$.
[e]Final total mass (leaves + stem + roots) of 5 harvested plants per growth temperature per provenance (g).
[f]Absolute growth rate during the 11-day growth interval (g $d^{-1}$).
[g]Relative growth rate during the 11-day growth interval (g $g^{-1}$ $d^{-1}$).
[h]Leaf area ratio averaged across the 11-day growth interval ($m^2$ $kg^{-1}$).
[i]Specific leaf area averaged across the 11-day growth interval ($cm^2$ $g^{-1}$).
[j]Light-saturated photosynthetic rates of plants measured at their in-situ growth temperature (μmol $CO_2$ $m^{-2}$ $s^{-1}$).
[k]Light-saturated photosynthetic rates of plants measured with short-term temperature response curves (μmol $CO_2$ $m^{-2}$ $s^{-1}$).

respiration (Figure 4d–f), particularly for leaves and roots. Notably, acclimation of $R_{stem}$ appeared to be homeostatic across the full range of measured growth temperatures (Figure 4b, e). These patterns were mostly equivalent across provenances, aside from a small difference for leaf respiration in the central provenance.

## 3.3 | Growth

We found no detectable differences between provenances from the cool-origin, central, or warm-origin of the distribution of *E. tereticornis* in the temperature responses of growth, measured either as the final mass of five destructively harvested individuals per provenance per treatment (Figure 5a), or the absolute growth rate (AGR) of 15 individuals per provenance per treatment during the 11-day growth interval (Figure 5b). The growth of all provenances was strongly temperature dependent and peaked at a mean 24-hour growth temperature of ~28°C (Figure 5). All provenances had equivalent temperature response parameters with overlapping 95% confidence intervals and NLMMs indicated no significant differences (Table 1). As with photosynthesis and respiration, these growth results reflect limited divergence in the thermal physiology for provenances across the range of this widely distributed species, consistent with hypothesis 2.

RGR during the 11-day interval also responded to growth temperature in a peaked fashion (Figure 6a) and all provenances had equivalent temperature response parameters with overlapping 95% confidence intervals (Table 1). Relative to AGR, RGR had a less pronounced peak and a lower $T_{opt}$. We decomposed RGR into the components of leaf area ratio (LAR) and net assimilation rate (NAR) via Equation (1). LAR increased with growth temperature until a peak at

**TABLE 2** Temperature-response parameter estimates and 95% confidence intervals for leaf dark respiration on a mass- and area-basis for three provenances of *E. tereticornis* based on Equation (3)

| Variable | Location | $R(T_{ref})$[a] | $Q_{10}$[b] |
|---|---|---|---|
| $R_{mass}$[c] | Cool-origin | 13.0 (11.9–14.2)$^A$ | 2.2 (1.8–2.5)$^A$ |
| $R_{mass}$ | Central | 13.1 (12.2–13.9)$^A$ | 2.2 (2.0–2.5)$^A$ |
| $R_{mass}$ | Warm-origin | 12.6 (11.5–13.7)$^A$ | 2.0 (1.7–2.3)$^A$ |
| $R_{area}$[d] | Cool-origin | 0.64 (0.60–0.69)$^A$ | 2.1 (1.8–2.4)$^A$ |
| $R_{area}$ | Central | 0.73 (0.68–0.78)$^A$ | 2.2 (2.0–2.5)$^A$ |
| $R_{area}$ | Warm-origin | 0.69 (0.66–0.72)$^A$ | 2.0 (1.8–2.1)$^A$ |

Statistically significant differences in parameters across provenances are indicated by different capital letters.

[a]Rate of respiration at the reference temperature of 22°C.

[b]Multiplicative change in respiration rate per 10°C change in temperature.

[c]Mass-based respiration rate (nmol $CO_2$ $g^{-1}$ $s^{-1}$).

[d]Area-based respiration rate (μmol $CO_2$ $m^{-2}$ $s^{-1}$).

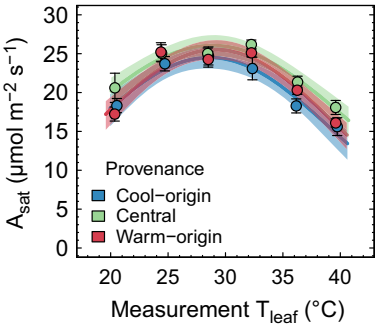


**FIGURE 3** The temperature response of leaf photosynthesis measured at the midday in-situ growth temperature and a high incident light of 1500 μmol $m^{-2}$ $s^{-1}$ ($A_{sat}$) for three provenances of *E. tereticornis*. Note that each plant was measured at its *in-situ* growth temperature, so these data reflect a long-term temperature response, rather than a short-term response. Points reflect the mean (±1*SE*, $n$ = 8), lines reflect functions fit to the data, and the shaded areas reflect 95% CI for the model predictions

~28°C and subsequently declined at the highest temperatures (Figure 6b). In contrast, NAR tended to decline with increasing growth temperature (Figure 6c). These results indicate that increasing leaf area display per unit plant mass (i.e., increased LAR) led to the initial increase in RGR at low temperatures, but that this effect was counterbalanced by reduced efficiency of dry mass production per unit leaf area as temperatures increased (i.e., reduced NAR). The relative strength of these two effects was modestly different across provenances, as the central provenance showed less temperature dependence in both LAR and NAR (Figure 6, Table 1).

Given the importance of LAR as a determinant of RGR, we decomposed LAR into its components of specific leaf area (SLA) and leaf mass fraction (LMF). SLA increased with temperature at low growth temperatures and subsequently declined at high growth temperatures (Figure 7a). In contrast, LMF was approximately constant at ~0.4 across the full range of temperatures, although LMF was reduced in the highest growth temperature (Figure 7b). The peaked response of SLA was coincident with a peaked response of average leaf size (Figure 7c) and an increase in total leaf number per seedling (Figure 7d). LAR was positively correlated with average leaf size across all observations (LAR = 9.5 + 0.28 × average leaf size, $r^2$ = .35, $p$ < .001). Collectively, these results suggest a strong effect of temperature on leaf expansion, such that warming at suboptimal temperatures increased the area of individual leaves, presumably increasing total seedling light interception and growth. At high temperatures, however, warming reduced the area of individual leaves and their efficiency of biomass production (NAR), leading to reduced growth. These patterns were equivalent for the cold- and warm-origin provenances; the central provenance showed moderate differences in LAR and SLA relative to the other provenances (Table 1), but had equivalent temperature dependencies of all growth metrics (final mass, AGR, and RGR).

These results provide new evidence that adds to the interpretation of our previous climate-shift experiment (Drake et al., 2015). The two experiments show a common temperature dependence of growth across 12 geographically diverse provenances of *E. tereticornis* with a $T_{opt}$ of ~28°C (Figure 8). Experimental warming increased the growth of provenances with a "home" temperature below $T_{opt}$, while warming reduced the growth of provenances with a "home" temperature exceeding $T_{opt}$. Thus, the differential effects of warming across broad geographic scales reported by Drake et al. (2015) primarily reflects the geographic gradient of "home" temperatures, rather than intrinsic differences across provenances.

## 4 | DISCUSSION

We found equivalent physiological and growth responses to temperature for contrasting cool-origin, central and warm-origin provenances of the widely distributed species *E. tereticornis*, consistent with the second hypothesis of a common thermal niche. The temperature dependence of growth was determined primarily by leaf size, specific leaf area (SLA), and the resulting impacts on leaf area per unit plant mass (LAR). Physiological acclimation of respiration dampened the increase in respiratory C loss with increasing temperature, but acclimation appeared to be constrained at high temperatures, resulting in higher rates of respiration and contributing to a reduction in whole-plant net assimilation rate (NAR) at high temperatures.

### 4.1 | A common thermal niche

Despite a ~2,200 km geographic distance and ~13°C difference in MAT among their sites of origin, these provenances had equivalent temperature responses of photosynthesis, respiration, and growth. These results suggest that *E. tereticornis* does not exhibit distinct genotypic and phenotypic variation associated with adaptation to climate-of-origin at broad geographic scales (i.e., hypothesis 1 was not supported). Provenances of this species appear to have a common set of phenotypes related to the temperature dependence of leaf

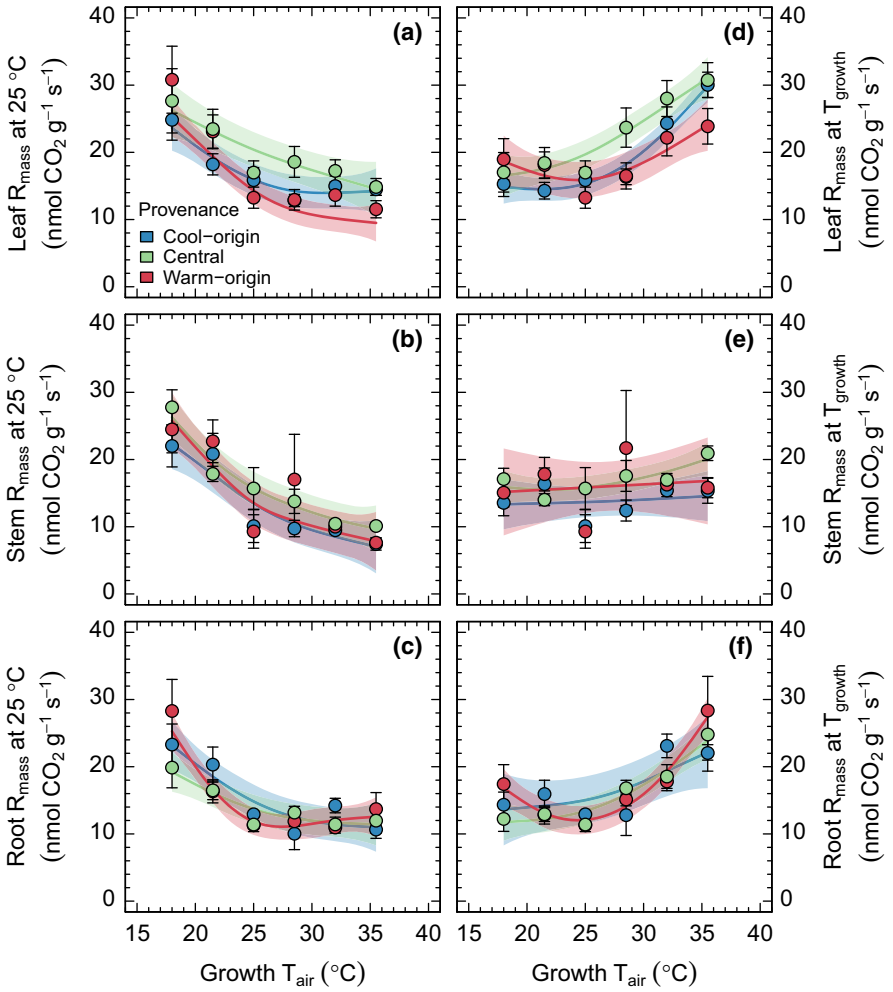


**FIGURE 4** Tissue-specific respiration rates at a common temperature of 25°C (a–c) and at the growth temperature (d–f) for three provenances of *E. tereticornis*. Leaf, stem, and root respiration rates were measured at 25°C and expressed per unit mass (a–c); values reflect the mean (±1*SE*) of five harvested plants per provenance per growth temperature; lines reflect general additive models fit to the data, and the shaded areas reflect 95% CI for the model predictions. Measurements at 25°C were used to estimate the rates of respiration at the in-situ growth environment temperature (d–f)

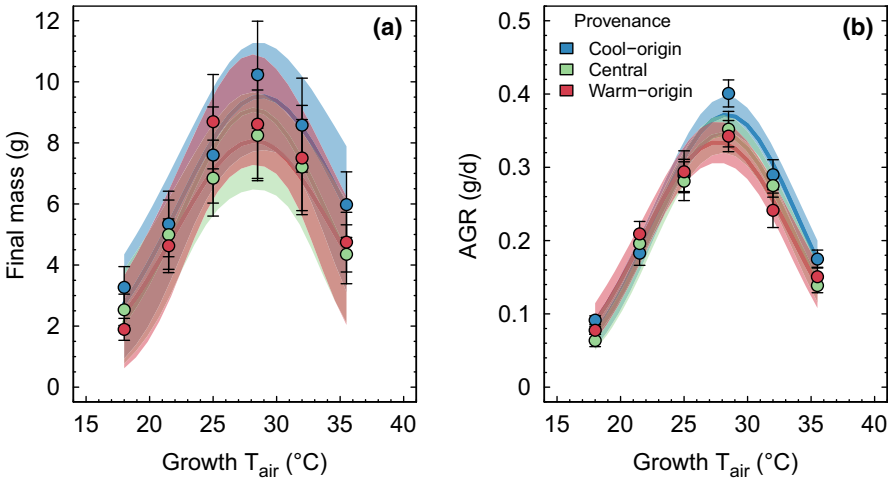


**FIGURE 5** Temperature response curves for final total plant mass (a); $n$ = 5, 45-day period and absolute growth rate during the 11-day measurement interval (b); $n$ = 15. Variables are plotted relative to the mean daily air temperature across the experiment. Lines reflect temperature response functions fit to the data and shaded areas reflect the 95% CI of the model predictions. The data are shown as circles; error bars reflect ±1*SE*

expansion, photosynthesis, and respiration, resulting in a common and broad temperature dependence of growth. These results are consistent with hypothesis 2.

These observed responses are surprising, as they contrast with evidence from widely distributed tree species from the Northern Hemisphere such as *Pinus sylvestris*, *P. contorta*, *Quercus spp.*, *Fagus sylvatica*, *Alnus glutinosa*, and the South American *Nothofagus pumilio*, which show strong provenance differences arrayed across clinal gradients (Fajardo & Piper, 2011; Newton, Allnutt, Gillies, Lowe, & Ennos, 1999; Rehfeldt et al., 1999, 2001, 2002; Reich & Oleksyn, 2008). Our results also contrast with *Eucalyptus pauciflora*, which shows strong provenance differences in growth and photosynthetic physiology arrayed along altitudinal gradients in the Snowy Mountains of Australia (Slatyer & Ferrar, 1977). Furthermore, a review of

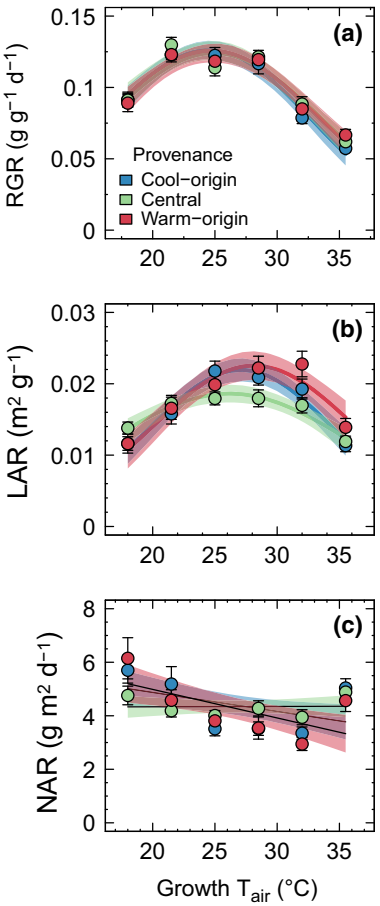


**FIGURE 6** Relative growth rate and its components derived from an 11-day measurement interval for three provenances of *E. tereticornis* trees grown at six temperatures. Points reflect the mean across the growth interval (±1*SE*; $n = 15$), lines reflect functions fit to the data, and the shaded areas reflect 95% CI for the model predictions. Relative growth rate (RGR; (a) is the product of leaf area ratio (LAR; (b) and the efficiency by which leaf area produces new biomass (net assimilation rate, or NAR; (c)

common garden experiments indicated that genetic differentiation across populations was found in approximately 90% of cases (Alberto et al., 2013). Thus, it would appear that our results for *E. tereticornis* are unusual. We suggest two possible reasons which alone or in combination could account for the lack of strong intraspecific differentiation in plant functional traits observed here: (i) the magnitude and importance of directional selection related to climate, and (ii) the level and maintenance of genetic variation, including long-distance gene flow.

Regarding (i), many of the widely distributed species with marked provenance differentiation inhabit cold environments crossing the boreal to cold-temperate climate regions, and at least some of the geographically structured intraspecific variation has been interpreted as adaptation to cold tolerance and the associated tradeoff with maximum growth rate (Reich, Oleksyn, & Tjoelker, 1996; Ögren, Nilsson, & Sundblad, 1997; Oleksyn, Modrzýnski, Tjoelker, Reich, & Karolewski, 1998; Ögren, 1999; Tjoelker, Oleksyn, Lorenc-Plucinska, & Reich, 2009). Strong intraspecific variation has also been demonstrated for snowgum (*E. pauciflora*) across altitudinal gradients in the Snowy Mountains of Australia (Slatyer & Ferrar, 1977). There are several reasons to think that cold tolerance may contribute a strong directional selection that may promote intraspecific genetic divergence. Many widespread trees use photoperiod as a cue to entrain budburst, shoot elongation and growth cessation to time periods when frost damage is minimized (Augspurger, 2013; Polgar & Primack, 2011; Vaartaja, 1959), and these phenological traits often manifest as genetic differences across provenances (Oleksyn, Tjoelker, & Reich, 1992; Howe et al., 2003; but see Chuine, Belmonte, & Mignot, 2000). However, *E. tereticornis* does not inhabit cold regions where cold-hardiness and frost-tolerance are expected to comprise a strong selection pressure; in fact, the species' distribution is nearly entirely constrained to environments where the mean minimum temperature of the coldest month exceeds 0°C (Figure 2b). Thus, we suggest that the lack of population divergence across the range of this species may partially be explained by a lack of strong directional selection associated with cold-tolerance, winter dormancy, and the need to entrain shoot and leaf production with photoperiod to minimize frost damage.

Regarding (ii), we suggest that long-distance gene-flow facilitated by bird and bat pollinators may act as a buffer against genetic divergence for provenances of *E. tereticornis* (reviewed by Southerton, Birt, Porter, & Ford, 2004). While insects are the primary visitor to *Eucalyptus* flowers in absolute number (House, 1997), birds are well-known as pollinators of *Eucalyptus spp.* in Australia, including honeyeaters (Meliphagidae), swift parrots (*Lathamus discolor*), and lorikeets (*Trichoglossus spp.*; Ford, Paton, & Forde, 1979; Southerton et al., 2004; Hingston, Gartrell, & Pinchbeck, 2004). Furthermore, at least four species of bats are known to feed on *Eucalyptus* nectar and have been observed visiting *E. tereticornis* flowers in southeastern Queensland, Australia (Barclay, 2002), and bats are known pollinators of many *Eucalyptus* and the closely related genus of *Corymbia* (Eby, 1995; Parry-Jones & Augee, 1991; Southerton et al., 2004). Many of these bats and birds migrate along the eastern coast of Australia and may facilitate long-distance pollination across the range of *E. tereticornis* (Southerton et al., 2004). While other processes maintaining high levels of local genetic variation may also be important, we hypothesize that long-distance pollination by birds and bats may have promoted genetic mixing within the widely distributed *E. tereticornis* and contributed to the lack of provenance divergence in physiology and growth responses to temperature.

## 4.2 | The temperature dependence of growth and respiration

Our observations of *E. tereticornis* suggest that the plasticity of leaf area display is the key determinant of the temperature dependence of RGR. The temperature dependence of RGR was primarily driven by LAR and SLA, while NAR and LMF had more limited impacts. The strong positive relationships between LAR, SLA, and average leaf size suggest that the rate of leaf expansion and final leaf size are important for LAR and thus the early growth of these seedlings.

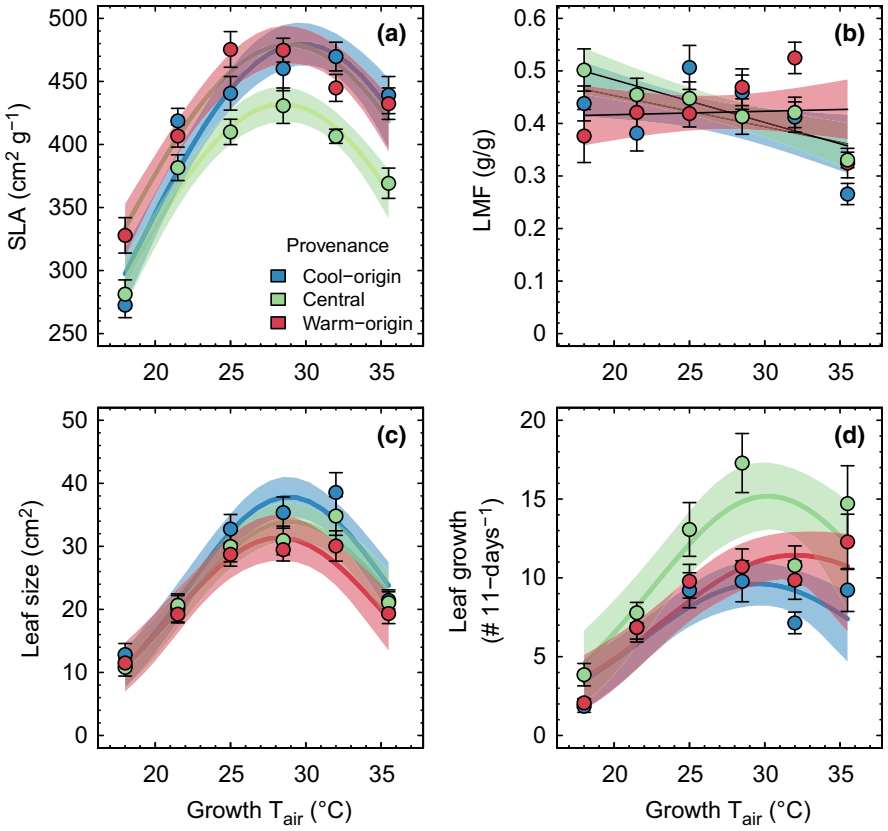


**FIGURE 7** Elements of leaf area ratio averaged across the 11-day measurement interval for three provenances of *E. tereticornis* grown at six temperatures. Points reflect the mean (±1*SE*; $n$ = 15), lines reflect functions fit to the data and shaded areas reflect the 95% confidence interval. Leaf area ratio is the product of specific leaf area (a) and leaf mass fraction (b). We also show the average size of individual leaves (c) and the average number of leaves produced per tree during the 11-day growth interval (d)

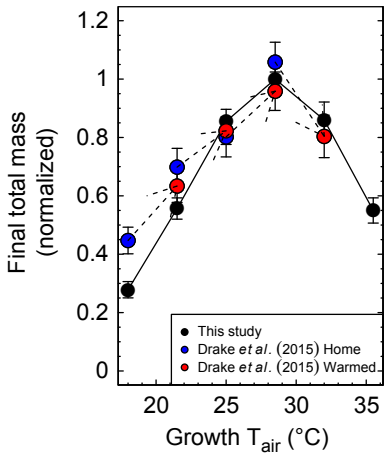


**FIGURE 8** A comparison of final biomass vs. growth temperature for two glasshouse experiments with *E. tereticornis*, illustrating that the effect of warming depends primarily on the "home" temperature. Final mass data were directly measured sums of leaf, stem, and root mass, normalized to the experiment-wise mean final mass at the peak growth temperature of 28.5°C, given the differences in tree mass across experiments of differing duration. Points reflect the mean of the normalized data and error bars reflect ±1*SE*. The data from this study reflect 15 observations per growth environment, while the data from Drake et al. (2015) reflect 12 provenances of contrasting "home" temperature, pooling 9 to 30 observations per growth environment. Drake et al. (2015) studied 12 provenances, each grown in two temperature environments ("home" and warmed by +3.5°C). Dashed arrows show the directional effect of +3.5°C warming for provenance home groups in the Drake et al. (2015) study

Temperature is known to directly influence cell division and expansion in developing leaves (Granier & Tardieu, 1998; Rymen et al., 2007; Savvides, van Ieperen, Dieleman, & Marcelis, 2016; Tardieu, Reymond, Hamard, Granier, & Muller, 2000). For *E. tereticornis*, the temperature effect on leaf development and growth may be most important during competition for canopy access after gap formation, which is an important component of the ecology of this species. We suggest that increasing mean daily temperatures up to ~28°C likely directly increased leaf development and LAR, leading to increasing growth. It is not clear whether the reduction in leaf size, LAR, and growth at temperatures exceeding ~28°C was caused directly by a deleterious effect of high temperature on development, or if physiological processes constrained C availability for leaf development at these high temperatures. While all trees were given abundant soil water, we recognize the possibility that aspects of water-relations may still have affected tree growth, particularly at high temperatures. Atmospheric vapor pressure deficit (VPD) increased with temperature (Fig. S1), which likely imposed a stomatal limitation to $A_{sat}$, increased transpiration rates, and in extreme cases, may have limited the rate of leaf expansion.

We suggest that the decline in growth at high temperature was at least partly driven by physiological constraints on C availability. Realized rates of light-saturated photosynthesis declined at high temperature while respiratory C loss increased. Remarkably, we found that leaves, stems, and roots all exhibited acclimation of respiration that was nearly homeostatic at growth temperatures from 18 to 25°C. Several recent studies have noted strong homeostatic acclimation of respiration to experimental warming (Aspinwall et al., 2016; Drake,

Tjoelker, et al., 2016; Reich et al., 2016), in contrast to weaker acclimation noted on average in prior studies (Slot & Kitajima, 2015). Our results also indicate that acclimation was markedly constrained at temperatures exceeding 25°C, especially for leaves and roots, such that whole-plant respiration increased at growth temperatures above the optimum. This observation of constrained acclimation at high temperature appears to be unusual. Slot and Kitajima (2015) summarized 43 studies of respiratory acclimation in response to experimental warming and found no detectable difference across biomes in the magnitude of acclimation and no trend regarding the magnitude of acclimation relative to maximum night-time temperatures. Thus, there is no general pattern of constrained acclimation to warming for plants inhabiting the tropical biome relative to temperate, boreal, or arctic plants (Slot & Kitajima, 2015). Our observations indicate that temperate and tropical provenances of *E. tereticornis* have equivalent capacity for respiratory acclimation, but that this capacity for acclimation appears to be constrained at high temperatures, perhaps owing to increased maintenance costs at higher temperatures. Our study explored a wider range of temperatures than any study summarized by Slot and Kitajima (2015), particularly at the hot extreme, which may explain why we observed a constraint on acclimation that was not present in the previous literature.

### 4.3 | Implications for climate warming responses

Our observation of a common fundamental thermal niche among contrasting provenances has implications for the predictions of how this widespread species may respond to climate change. Our work implies that such predictions are not likely to be strongly influenced by spatial patterns of underlying genetic differences in this species. Quite simply, warming temperatures are likely to directly benefit growth in relatively cold environments but reduce growth in warm environments.

However, increased temperatures are likely to be accompanied by other effects in field conditions that may constrain or alter this direct temperature response, including nutrient limitations, altered water availability, competition from other plants, and herbivory and pathogen attack. For example, the radial growth of *Eucalyptus* trees in the field has a low temperature optimum of ~11°C MAT, which may be influenced by the negative relationship between MAT and water availability (Bowman, Williamson, Keenan, & Prior, 2014), such that water limitation may constrain a positive growth response to warming, even at suboptimal temperatures (but see Prior & Bowman, 2014). Environmental and biotic interactions likely constrain the realized niche of adult trees relative to the fundamental niche studied here. Furthermore, we note that some studies found aspects of allometry and biomass allocation to be important components related to geographic patterns in tree function across populations of widely distributed species (Oleksyn et al., 1998; Mencuccini & Bonosi, 2001). These aspects of local adaptation in whole-tree processes would not necessarily be reflected in our study of potted trees in controlled environments.

We found equivalent temperature responses of photosynthesis, respiration, and growth for three provenances of *E. tereticornis*, despite a ~2200 km geographic distance and a ~13°C difference in MAT at their sites of origin. The peaked and broad temperature dependence of growth was strongly influenced by leaf expansion and the resulting leaf area per unit plant mass (LAR). Acclimation of respiration reduced C losses with increasing temperature in a way that likely moderated the temperature dependence of net assimilation rate (NAR), but respiratory acclimation appeared to be constrained at high temperatures. We conclude that a common set of functional traits related to leaf area and its physiological function define a broad and equivalent thermal niche across the geographic range of this widely distributed species.

## ACKNOWLEDGEMENTS

We thank Goran Lopaticki, Burhan Amiji, and Gavin Mckenzie (Western Sydney University; WSU) for their technical assistance with the glasshouse facility. We thank Mike Aspinwall (WSU) for his many conceptual contributions to this work. We thank Rosana López (WSU) for measuring and providing the pre-dawn leaf water potential data. This research was supported by an Australian Research Council Discovery Project grant (DP140103415) with additional support from the Hawkesbury Institute for the Environment and Western Sydney University. We acknowledge the contributions of five anonymous reviewers, whose comments and criticisms improved this work.

## 5 | AUTHORSHIP STATEMENT

JED led the experimental design, data collection, analysis, and writing of this project. AV was the technical lead on the experimental implementation, and she contributed to the experimental design, data collection, and writing. DK collected data and contributed to the analysis and writing. BEM contributed to the experimental design, data analysis and interpretation, and writing. SP, DTT, PBR, and OM contributed to the experimental design and/or writing. MGT was the senior scientific lead on the project; he contributed to data collection and made a substantial contribution to the experimental design, data interpretation, and writing.

## REFERENCES

Alberto, F. J., Aitken, S. N., Alía, R., González Martínez, S. C., Hänninen, H., Kremer, A., ... Savolainen, O. (2013). Potential for evolutionary responses to climate change–evidence from tree populations. *Global Change Biology*, *19*, 1645–1661.

Aspinwall, M. J., Drake, J. E., Campany, C., Vårhammar, A., Ghannoum, O., Tissue, D. T., ... Tjoelker, M. G. (2016). Convergent acclimation of leaf photosynthesis and respiration to prevailing ambient temperatures under current and warmer climates in *Eucalyptus tereticornis*. *New Phytologist*, *212*, 354–367.

Atkin, O. K., Bloomfield, K. J., Reich, P. B., Tjoelker, M. G., Asner, G. P., Bonal, D., ... Zaragoza-Castells, J. (2015). Global variability in leaf respiration in relation to climate, plant functional types and leaf traits. *New Phytologist*, *206*, 614–636.

Atkin, O. K., Bruhn, D., & Tjoelker, M. G. (2005). Response of plant respiration to changes in temperature: Mechanisms and consequences of variations in $Q_{10}$ values and acclimation. In H. Lambers, & M. Ribas-

Carbo (Eds.), *Plant respiration* (pp. 95–135). The Netherlands: Springer.

Augspurger, C. K. (2013). Reconstructing patterns of temperature, phenology, and frost damage over 124 years: Spring damage risk is increasing. *Ecology*, *94*, 41–50.

Barclay, R. M. (2002). Do plants pollinated by flying fox bats (Megachiroptera) provide an extra calcium reward in their nectar? 1. *Biotropica*, *34*, 168–171.

Baty, F., Ritz, C., Charles, S., Brutsche, M., Flandrois, J. P., & Delignette-Muller, M. L. (2015). A toolbox for nonlinear regression in R: The package nlstools. *Journal of Statistical Software*, *66*, 1–21.

Bolstad, P. V., Reich, P., & Lee, T. (2003). Rapid temperature acclimation of leaf respiration rates in *Quercus alba* and *Quercus rubra*. *Tree Physiology*, *23*, 969–976.

Booth, T. H., Broadhurst, L. M., Pinkard, E., Prober, S. M., Dillon, S. K., Bush, D., … Young, A. G. (2015). Native forests and climate change: Lessons from eucalypts. *Forest Ecology and Management*, *347*, 18–29.

Bowman, D. M. J. S., Williamson, G. J., Keenan, R. J., & Prior, L. D. (2014). A warmer world will reduce tree growth in evergreen broadleaf forests: Evidence from Australian temperate and subtropical eucalypt forests. *Global Ecology and Biogeography*, *23*, 925–934.

Busby, J. (1991). BIOCLIM-a bioclimate analysis and prediction system. *Plant Protection Quarterly (Australia)*, *6*, 8–9.

Chuine, I., Belmonte, J., & Mignot, A. (2000). A modelling analysis of the genetic variation of phenology between tree populations. *Journal of Ecology*, *88*, 561–570.

Collins, M., Knutti, R., Arblaster, J., Dufresne, J.-L., Fichefet, T., Friedlingstein, P., … Wehner, M. (2013). Long-term climate change: Projections, commitments and irreversibility. In T. F. Stocker, D. Qin, G. K. Plattner, M. Tignor, S. K. Allen, J. Boschung, A. Nauels, Y. Xia, V. Bex & P. M. Midgley (Eds.), *Climate change 2013: The physical science basis. Contribution of Working Group I to the Fifth Assessment Report of the Intergovernmental Panel on Climate Change* (pp. 1030–1107). Cambridge, UK and New York, NY, USA: Cambridge University Press.

Comas, L. H., & Eissenstat, D. M. (2004). Linking fine root traits to maximum potential growth rate among 11 mature temperate tree species. *Functional Ecology*, *18*, 388–397.

Davey, P. A., Hunt, S., Hymus, G. J., Delucia, E. H., Drake, B. G., Karnosky, D. F., & Long, S. P. (2004). Respiratory oxygen uptake is not decreased by an instantaneous elevation of $CO_2$, but is increased with long-term growth in the field at elevated $CO_2$ (1). *Plant Physiology*, *134*, 520–527.

Davis, M. B., & Shaw, R. G. (2001). Range shifts and adaptive responses to Quaternary climate change. *Science*, *292*, 673–679.

Dillon, S., McEvoy, R., Baldwin, D. S., Rees, G. N., Parsons, Y., & Southerton, S. (2014). Characterisation of adaptive genetic diversity in environmentally contrasted populations of *Eucalyptus camaldulensis* Dehnh. (River Red Gum). *PLoS ONE*, *9*, e103515.

Doak, D. F., & Morris, W. F. (2010). Demographic compensation and tipping points in climate-induced range shifts. *Nature*, *467*, 959–962.

Drake, J. E., Aspinwall, M. J., Pfautsch, S., Rymer, P. D., Reich, P. B., Smith, R. A., … Tjoelker, M. G. (2015). The capacity to cope with climate warming declines from temperate to tropical latitudes in two widely distributed Eucalyptus species. *Global Change Biology*, *21*, 459–472.

Drake, J. E., Tjoelker, M. G., Aspinwall, M. J., Reich, P. B., Barton, C. V. M., Medlyn, B. E., & Duursma, R. A. (2016). Does physiological acclimation to climate warming stabilize the ratio of canopy respiration to photosynthesis? *New Phytologist*, *211*, 850–863.

Drake, J. E., Vårhammar, A., Kumarathunge, D., Medlyn, B. E., Pfautsch, S., & Tjoelker, M. G. (2016). *Growth, leaf photosynthesis, leaf stem and root respiration, temperature, humidity, and photosynthetic photon flux density data for a glasshouse temperature experiment with Eucalyptus tereticornis*. Penrith, NSW: Western Sydney University. http://doi.org/10.4225/35/57e4bf22dd3ec

Eby, P. (1995). *The biology and management of flying foxes in New South Wales*. Hurstville, NSW, USA: NSW National Parks and Wildlife Service.

Fajardo, A., & Piper, F. I. (2011). Intraspecific trait variation and covariation in a widespread tree species (*Nothofagus pumilio*) in southern Chile. *New Phytologist*, *189*, 259–271.

Ford, H. A., Paton, D. C., & Forde, N. (1979). Birds as pollinators of Australian plants. *New Zealand Journal of Botany*, *17*, 509–519.

Gauli, A., Vaillancourt, R. E., Bailey, T. G., Steane, D. A., & Potts, B. M. (2015). Evidence for local climate adaptation in early-life traits of Tasmanian populations of *Eucalyptus pauciflora*. *Tree Genetics & Genomes*, *11*, 1–14.

González-Orozco, C. E., Pollock, L. J., Thornhill, A. H., Mishler, B. D., Knerr, N., Laffan, S. W., … Gruber, B. (2016). Phylogenetic approaches reveal biodiversity threats under climate change. *Nature Climate Change*, *6*, 1110–1114.

Granier, C., & Tardieu, F. (1998). Is thermal time adequate for expressing the effects of temperature on sunflower leaf development? *Plant, Cell & Environment*, *21*, 695–703.

Heskel, M. A., O'Sullivan, O. S., Reich, P. B., Tjoelker, M. G., Weerasinghe, L. K., Penillard, A., … Atkin, O. K. (2016). Convergence in the temperature response of leaf respiration across biomes and plant functional types. *Proceedings of the National Academy of Sciences*, *113*, 3832–3837.

Hingston, A. B., Gartrell, B. D., & Pinchbeck, G. (2004). How specialized is the plant–pollinator association between *Eucalyptus globulus* ssp. *globulus* and the swift parrot *Lathamus discolor*? *Austral Ecology*, *29*, 624–630.

House, S. (1997). Reproductive biology of eucalypts. In J. Williams, & J. Woinarski (Eds.), *Eucalypt ecology: Individuals to ecosystems* (pp. 30–55). Cambridge: Cambridge University Press.

Howe, G. T., Aitken, S. N., Neale, D. B., Jermstad, K. D., Wheeler, N. C., & Chen, T. H. H. (2003). From genotype to phenotype: Unraveling the complexities of cold adaptation in forest trees. *Canadian Journal of Botany*, *81*, 1247–1266.

Jump, A. S., & Penuelas, J. (2005). Running to stand still: Adaptation and the response of plants to rapid climate change. *Ecology Letters*, *8*, 1010–1020.

June, T., Evans, J. R., & Farquhar, G. D. (2004). A simple new equation for the reversible temperature dependence of photosynthetic electron transport: A study on soybean leaf. *Functional Plant Biology*, *31*, 275–283.

Kirschbaum, M. U. (2011). Does enhanced photosynthesis enhance growth? Lessons learned from $CO_2$ enrichment studies. *Plant Physiology*, *155*, 117–124.

Langlet, O. (1936). Studies on the physiological variability of Scots Pine and its relation to climate. *Meddelanden från statens skogsförsöksanstalt*, *29*, 219–406.

Loarie, S. R., Duffy, P. B., Hamilton, H., Asner, G. P., Field, C. B., & Ackerly, D. D. (2009). The velocity of climate change. *Nature*, *462*, 1052–1055.

Mencuccini, M., & Bonosi, L. (2001). Leaf/sapwood area ratios in Scots pine show acclimation across Europe. *Canadian Journal of Forest Research*, *31*, 442–456.

McLean, E. H., Prober, S. M., Stock, W. D., Steane, D. A., Potts, B. M., Vaillancourt, R. E., & Byrne, M. (2014). Plasticity of functional traits varies clinally along a rainfall gradient in *Eucalyptus tricarpa*. *Plant, Cell & Environment*, *37*, 1440–1451.

Mitchell, K. A., Bolstad, P. V., & Vose, J. M. (1999). Interspecific and environmentally induced variation in foliar dark respiration among eighteen southeastern deciduous tree species. *Tree Physiology*, *19*, 861–870.

Moran, G. (1992). Patterns of genetic diversity in Australian tree species. *New Forests*, *6*, 49–66.

Newton, A., Allnutt, T., Gillies, A., Lowe, A., & Ennos, R. (1999). Molecular phylogeography, intraspecific variation and the conservation of tree species. *Trends in Ecology & Evolution*, *14*, 140–145.

Ögren, E. (1999). Fall frost resistance in willows used for biomass production. II. Predictive relationships with sugar concentration and dry matter content. *Tree Physiology*, *19*, 755–760.

Ögren, E., Nilsson, T., & Sundblad, L. (1997). Relationship between respiratory depletion of sugars and loss of cold hardiness in coniferous seedlings over-wintering at raised temperatures: Indications of different sensitivities of spruce and pine. *Plant, Cell & Environment*, *20*, 247–253.

Oleksyn, J., Modrzýnski, J., Tjoelker, M.G., Reich, P. B., & Karolewski, P. (1998). Growth and physiology of *Picea abies* populations from elevational transects: Common garden evidence for altitudinal ecotypes and cold adaptation. *Functional Ecology*, *12*, 573–590.

Oleksyn, J., Tjoelker, M. G., & Reich, P. B. (1992). Growth and biomass partitioning of populations of European *Pinus sylvestris* L. under simulated 50° and 60° N daylengths: Evidence for photoperiodic ecotypes. *New Phytologist*, *120*, 561–574.

O'Sullivan, O. S., Weerasinghe, K. L. K., Evans, J. R., Egerton, J. J., Tjoelker, M. G., & Atkin, O. K. (2013). High-resolution temperature responses of leaf respiration in snow gum (*Eucalyptus pauciflora*) reveal high-temperature limits to respiratory function. *Plant, Cell & Environment*, *36*, 1268–1284.

Parmesan, C. (2006). Ecological and evolutionary responses to recent climate change. *Annual Review of Ecology, Evolution, and Systematics*, *37*, 637–669.

Parry-Jones, K. A., & Augee, M. (1991). Food selection by grey-headed flying-foxes *(Pteropus poliocephalus)* occupying a summer colony site near Gosford, New South Wales. *Wildlife Research*, *18*, 111–124.

Polgar, C. A., & Primack, R. B. (2011). Leaf-out phenology of temperate woody plants: From trees to ecosystems. *New Phytologist*, *191*, 926–941.

Poorter, H., Remkes, C., & Lambers, H. (1990). Carbon and nitrogen economy of 24 wild species differing in relative growth rate. *Plant Physiology*, *94*, 621–627.

Potts, B. M., & Wiltshire, R. J. E. (1993). Eucalypt genetics and genecology. In K. Eldridge, J. Davidson, C. Harwood & G. WYK (Eds.), *Eucalypt domestication and breeding* (pp. 56–91). Oxford: Clarendon press.

Prior, L. D., & Bowman, D. M. J. S. (2014). Big eucalypts grow more slowly in a warm climate: Evidence of an interaction between tree size and temperature. *Global Change Biology*, *20*, 2793–2799.

R Development Core Team. (2012). *R: A language and environment for statistical computing*. Vienna, Austria: R Foundation for Statistical Computing.

Rehfeldt, G. E., Tchebakova, N. M., Parfenova, Y. I., Wykoff, W. R., Kuzmina, N. A., & Milyutin, L. I. (2002). Intraspecific responses to climate in *Pinus sylvestris*. *Global Change Biology*, *8*, 912–929.

Rehfeldt, G. E., Wykoff, W. R., & Ying, C. C. (2001). Physiologic plasticity, evolution, and impacts of a changing climate on *Pinus contorta*. *Climatic Change*, *50*, 355–376.

Rehfeldt, G. E., Ying, C. C., Spittlehouse, D. L., & Hamilton, D. A. (1999). Genetic responses to climate in *Pinus contorta*: Niche breadth, climate change, and reforestation. *Ecological Monographs*, *69*, 375–407.

Reich, P. B., & Oleksyn, J. (2008). Climate warming will reduce growth and survival of Scots pine except in the far north. *Ecology Letters*, *11*, 588–597.

Reich, P.B., Oleksyn, J., & Tjoelker, M. G. (1996). Needle respiration and nitrogen concentration in Scots pine populations from a broad latitudinal range: A common garden test with field-grown trees. *Functional Ecology*, *10*, 768–776.

Reich, P. B., Sendall, K. M., Stefanski, A., Wei, X., Rich, R. L., & Montgomery, R. A. (2016). Boreal and temperate trees show strong acclimation of respiration to warming. *Nature*, *531*, 633–636.

Reich, P. B., Walters, M. B., Ellsworth, D. S., Vose, J. M., Volin, J. C., Gresham, C., & Bowman, W. D. (1998). Relationships of leaf dark respiration to leaf nitrogen, specific leaf area and leaf life-span: A test across biomes and functional groups. *Oecologia*, *114*, 471–482.

Rymen, B., Fiorani, F., Kartal, F., Vandepoele, K., Inze, D., & Beemster, G. T. S. (2007). Cold nights impair leaf growth and cell cycle progression in maize through transcriptional changes of cell cycle genes. *Plant Physiology*, *143*, 1429–1438.

Savvides, A., van Ieperen, W., Dieleman, J. A., & Marcelis, L. F. M. (2016). Phenotypic plasticity to altered apical bud temperature in *Cucumis sativus*: More leaves-smaller leaves and vice versa. *Plant, Cell & Environment*, *40*, 69–79.

Shipley, B. (2006). Net assimilation rate, specific leaf area and leaf mass ratio: Which is most closely correlated with relative growth rate? A meta-analysis. *Functional Ecology*, *20*, 565–574.

Slatyer, R. O., & Ferrar, P. J. (1977). Altitudinal variation in the photosynthetic characteristics of snow gum, *Eucalyptus pauciflora* Sieb. ex Spreng. II. Effects of growth temperature under controlled conditions. *Australian Journal of Plant Physiology*, *4*, 289–299.

Slot, M., & Kitajima, K. (2015). General patterns of acclimation of leaf respiration to elevated temperatures across biomes and plant types. *Oecologia*, *177*, 885–900.

Southerton, S., Birt, P., Porter, J., & Ford, H. (2004). Review of gene movement by bats and birds and its potential significance for eucalypt plantation forestry. *Australian Forestry*, *67*, 44–53.

Tardieu, F., Reymond, M., Hamard, P., Granier, C., & Muller, B. (2000). Spatial distributions of expansion rate, cell division rate and cell size in maize leaves: A synthesis of the effects of soil water status, evaporative demand and temperature. *Journal of Experimental Botany*, *51*, 1505–1514.

Tjoelker, M. G., Craine, J. M., Wedin, D., Reich, P. B., & Tilman, D. (2005). Linking leaf and root trait syndromes among 39 grassland and savannah species. *New Phytologist*, *167*, 493–508.

Tjoelker, M. G., Oleksyn, J., & Reich, P. B. (1999). Acclimation of respiration to temperature and $CO_2$ in seedlings of boreal tree species in relation to plant size and relative growth rate. *Global Change Biology*, *5*, 679–691.

Tjoelker, M. G., Oleksyn, J., & Reich, P. B. (2001). Modelling respiration of vegetation: Evidence for a general temperature-dependent $Q_{10}$. *Global Change Biology*, *7*, 223–230.

Tjoelker, M. G., Oleksyn, J., Lorenc-Plucinska, G., & Reich, P. B. (2009). Acclimation of respiratory temperature responses in northern and southern populations of *Pinus banksiana*. *New Phytologist*, *181*, 218–229.

Vaartaja, O. (1959). Evidence of photoperiodic ecotypes in trees. *Ecological Monographs*, *29*, 91–111.

Valladares, F., Matesanz, S., Guilhaumon, F., Araújo, M. B., Balaguer, L., Benito-Garzón, M., … Zavala, M. A. (2014). The effects of phenotypic plasticity and local adaptation on forecasts of species range shifts under climate change. *Ecology Letters*, *17*, 1351–1364.

Woodward, F. I. (1987). *Climate and plant distribution*. Cambridge: Cambridge University Press.

## SUPPORTING INFORMATION

Additional Supporting Information may be found online in the supporting information tab for this article.

**How to cite this article:** Drake JE, Vårhammar A, Kumarathunge D, et al. A common thermal niche among geographically diverse populations of the widely distributed tree species *Eucalyptus tereticornis*: No evidence for adaptation to climate-of-origin. *Glob Change Biol*. 2017;23:5069–5082. https://doi.org/10.1111/gcb.13771

**Supplemental information**

Article title: A common thermal niche among geographically diverse populations of the widely distributed tree species *Eucalyptus tereticornis*: no evidence for adaptation to climate of origin

Authors: John E. Drake, Angelica Vårhammar, Dushan Kumarathunge, Belinda E. Medlyn, Sebastian Pfautsch, Peter B. Reich, David T. Tissue, Oula Ghannoum, Mark G. Tjoelker

The following Supporting Information is available for this article:

**Fig. S1** Environmental data observed inside six glasshouse bays at Western Sydney University in 2016. Mean daily values of air temperature ($T_{air}$; a), relative humidity (RH; b), and vapor pressure deficit (VPD; c) are shown along with hourly averages of incident photosynthetic photon flux density (PPFD; d). Six colors are shown; cool colors reflect low temperature bays while hot colors reflect high temperature bays. PPFD did not differ across bays, so we present the mean PPFD for clarity. Note that there was substantial diurnal variation in $T_{air}$, RH, and VPD that is not evident in these plots of 24-hour averages.

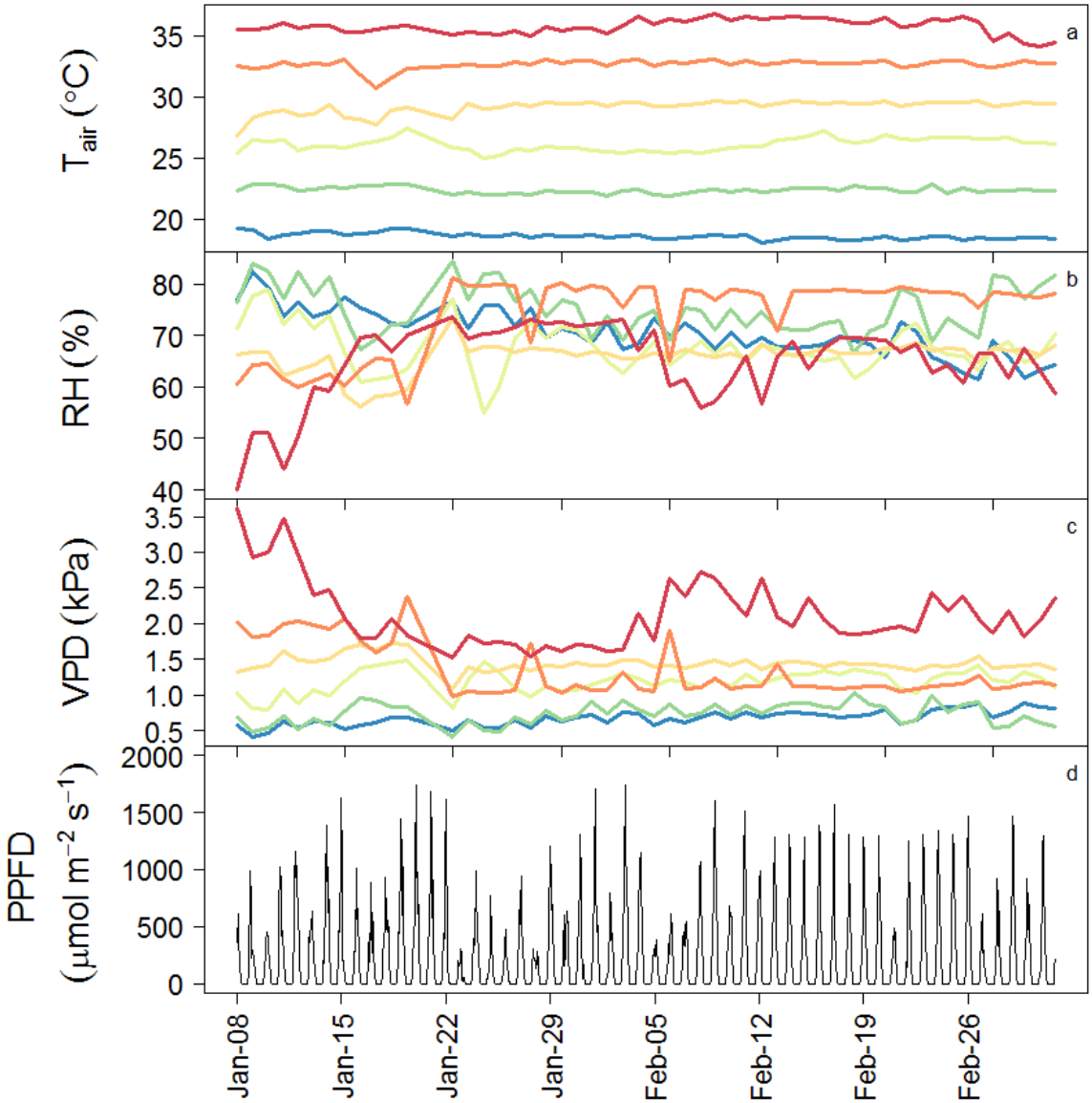

**Fig. S2** Allometry relating a metric of plant size with total mass for 156 harvested plants of three provenances of *Eucalyptus tereticornis*. Total mass reflects the measured sum of leaf, stem (including branches) and root mass; $d^2h$ reflects the square of stem diameter multiplied by height. Both variables were $\log_{10}$ transformed. The line reflects a second-order polynomial fit to the data ($y = -0.018 + 0.85x - 0.064x^2$; $r^2 = 0.98$).

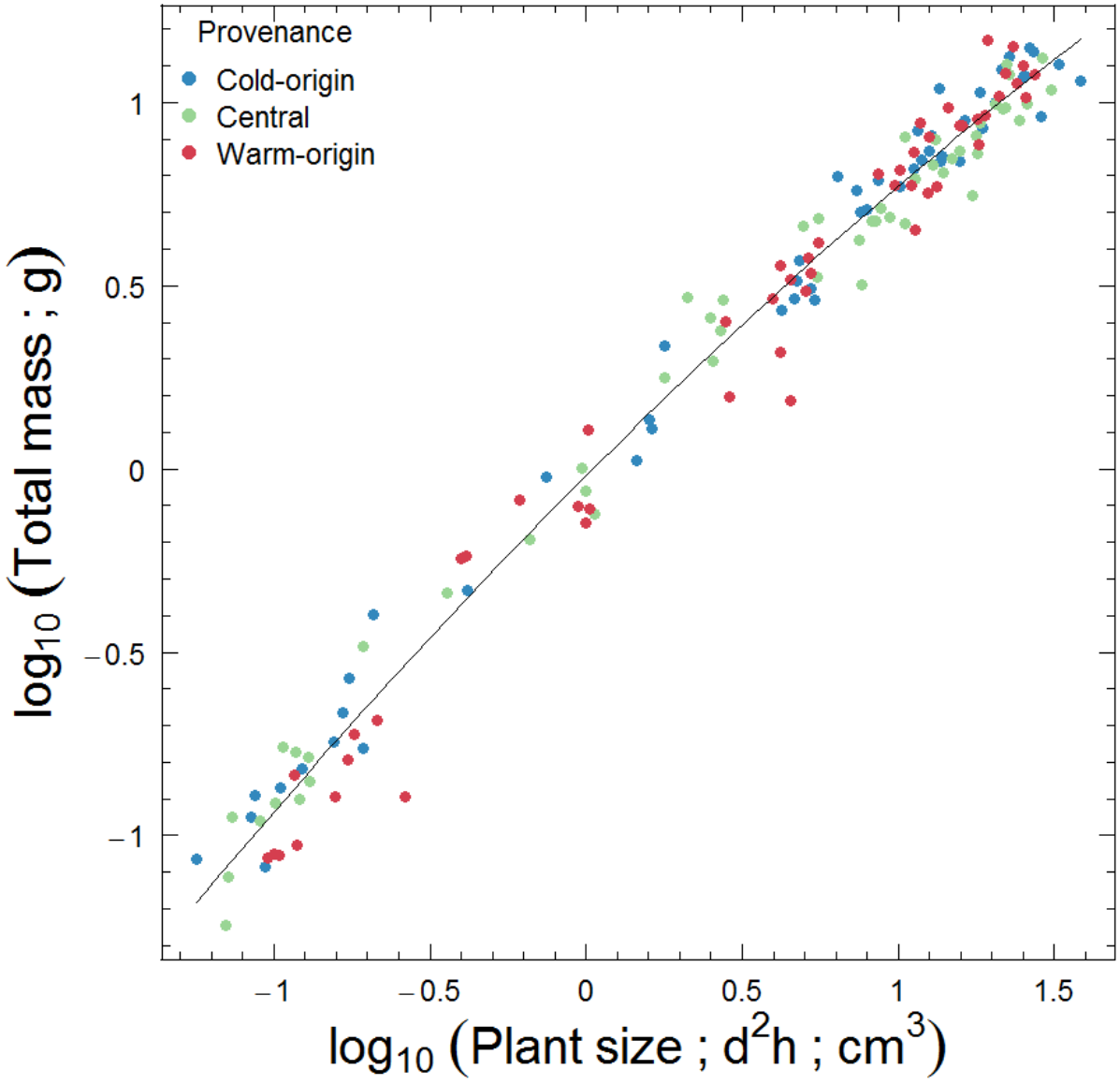

**Fig. S3** The direct short-term temperature response of leaf light saturated photosynthesis ($A_{sat}$) per unit leaf area (a) or per unit mass (b) for three provenances of *Eucalyptus tereticornis* grown in a common environment (mean temperature of 21.5°C). Points reflect the mean (±1SE), lines reflect functions fit to the data, and the shaded areas reflect 95% CI for the model predictions. Rank differences across provenances between area-based and mass-based rates reflect differences in the specific leaf area of the measurement leaves.

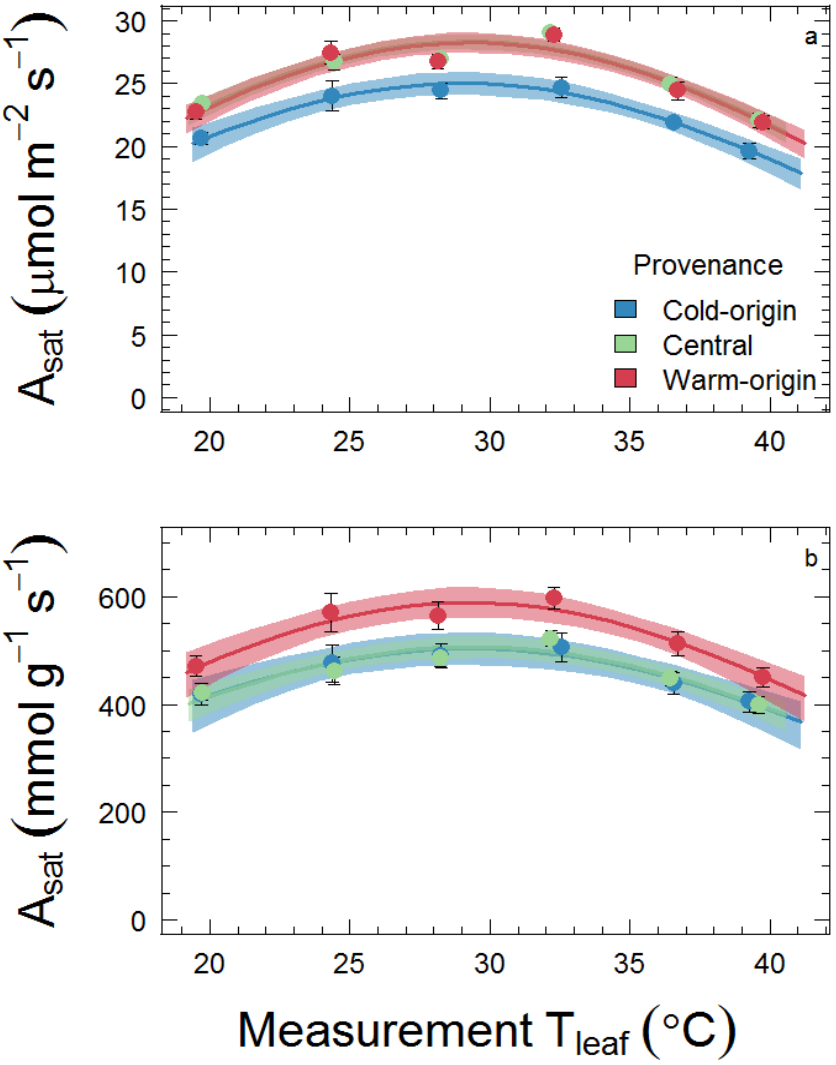

**Fig. S4** The direct short-term temperature response of leaf respiration in the dark per unit leaf mass (a) or per unit area (b) for three provenances of *Eucalyptus tereticornis* grown in a common environment (mean temperature of 21.5°C). Points reflect the mean (±1SE), lines reflect functions fit to the data, and the shaded areas reflect 95% CI for the model predictions.